Image Cover Sheet

CLASSIFICATION	SYSTEM NUMBER
UNCLASSIFIED	508292

TITLE

THE INTERACTION DYNAMICS OF A SEMI-SUBMERSIBLE TOWING A LARGE TOWFISH

System Number:

Patron Number:

Requester:

Notes:

DSIS Use only:

Deliver to:

Proceedings of the Eighth (1998) International Offshore and Polar Engineering Conference
Montréal, Canada, May 24-29, 1998

ISBN 1-880653-34-6 (Set); ISBN 1-880653-36-2 (Vol. II)

The Interaction Dynamics of a Semi-Submersible Towing a Large Towfish

Mae L. Seto
International Submarine Engineering Research Ltd.
Port Coquitlam, Canada

George D. Watt
Defence Research Establishment Atlantic
Dartmouth, Canada

ABSTRACT

The interactions between a semi-submersible drone and its large towfish, where the tension in the tow cable joining them is about 20% of the weight of the drone, are investigated. Since standard cable dynamics modelling computer programs do not model tow-vehicle/tow-body interactions, an iterative approach to calculating these interactions is developed. Drone motions are modelled with a non-linear, six degree-of-freedom, underwater vehicle simulation incorporating pre-defined, three component, time dependent tow cable tensions applied at the tow point. Cable dynamics are modelled with the non-linear, finite segment, cable/towfish dynamic simulator DYNTOCABS, which accepts pre-defined tow-point accelerations as time varying boundary conditions. The interactions are calculated by iterating between these two programs. The method is applied to simple turning maneuvers important to minehunting operations.

KEY WORDS: Cable Dynamics, Towfish, Semi-Submersible, Coupled Motions, Interactions

NOMENCLATURE

D	diameter of turn.
i	iteration index.
ℓ	drone length.
m, m'	drone mass; $m' = m/(\frac{1}{2}\rho\ell^3)$.
N'_r	yaw moment due to yaw rate.
N'_v	yaw moment due to lateral velocity.
$N'_{\delta r}$	yaw moment due to rudder deflection.
r, r'	yaw rate; $r' = r\ell/U$.
rpm	revolutions per minute.
t_s	time, in a U-turn, at which the rudder is re-zeroed.
T'_y	lateral body reference frame tension.
U	drone speed.
x_G, x'_G	drone longitudinal center of gravity; $x'_G = x_G/\ell$.
x_t, x'_t	longitudinal location of cable towpoint on drone.
X, Y, Z	inertial reference frame displacement coordinates.
Y'_r	lateral force due to yaw rate.
Y'_v	lateral force due to lateral velocity.
$Y'_{\delta r}$	lateral force due to rudder deflection.
$\delta_{r,i}$	i^{th} iteration rudder deflection.
ψ	drone heading.
ψ_f	final drone heading after a manoeuvre.
θ	drone pitch.
ϕ	drone roll.

Primed quantities are dimensionless. Forces are nondimensionalized with $\rho U^2\ell^2/2$, and moments with $\rho U^2\ell^3/2$, where ρ is the density of sea water.

1. INTRODUCTION

DREA and ISER are evaluating issues facing the development of a Canadian Remote Minehunting System (CRMS) for the Canadian Navy. The CRMS is an autonomous, snorkelling drone towing a deployable, active towfish which houses a side scan sonar for route surveying and mine location on the sea floor. With route surveying, sonar images are obtained from an area where mine hunting is anticipated, in order to provide a reference against which future mine hunting images can be compared. A high degree of towfish stability is required to get good images, and the absolute location of the towfish must be known for differencing images with those from subsequent mine hunting surveys. Drone motions, whether from waves or necessary maneuvers, cause towfish (sonar) disturbances. These disturbances degrade the sonar image and make mine detection and classification difficult.

The requirement for high towfish stability leads to a need for a stable towing platform. The semi-submersible DOLPHIN (Deep Ocean Logging Platform for Hydrographic Instrumentation and Navigation) Mk1 vehicle developed by ISE Research Ltd. is a proven stable remote platform for hydrographic instrumentation. It can operate in up to sea state 5 and has successfully demonstrated its towing capability (Preston and Shupe, 1993). DOLPHIN Mk2 (Figure 1) is currently a candidate drone for the CRMS. It is 8.5 m long with a 1 m hull diameter, has a

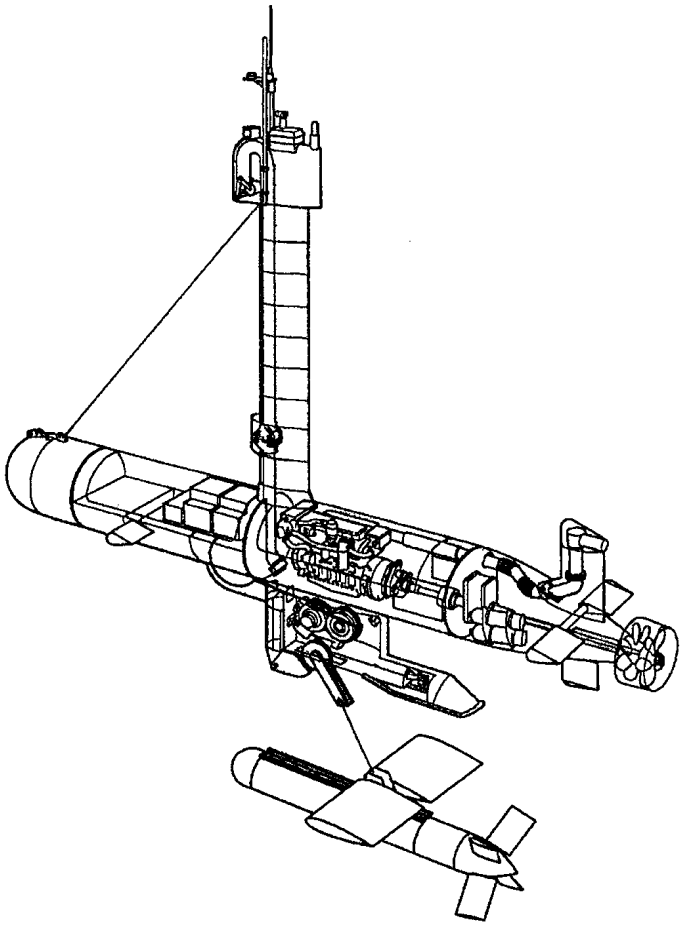

Fig. 1 *DOLPHIN Mk2 and towfish.*

dry mass of 4500 kg, and uses a 350 horsepower engine to drive contra-rotating propellers. The towfish considered in this study (Figure 1) is 3.2 m in length with a 0.5 m diameter hull. It has a dry mass of 445 kg, an active depressor with a 2.4 m span, and four symmetrical, independently active tailfins.

A semi-submersible minehunting drone has personnel safety and cost advantages over a minehunting surface ship, yet retains the larger ship's stability in waves, its air breathing endurance, high data rate real time communications link, and accurate global positioning characteristics. The drone is, however, still subject to surge motions in high sea states and these result in cyclic tow cable tension and, potentially, towfish positioning variations. Also, the lower inertia of the drone results in increased interactions with the towfish and cable. The cable tensions with a towfish depressed to 100 m depth with 300 m of scope can be 20% of the weight of the drone.

Therefore, there is a need to assess the impact of both drone motions on the tow system and the tow system response on the maneuverability of the drone. The dynamics of maneuvering with towed systems have been studied by many workers (Chapman, 1984; Henry, 1985; Duvat and Large, 1997) who have looked at turning maneuvers and how to minimize their impact on the ship (Le Guerch, 1987) or the towfish displacement (Chapman, 1984). Ship induced motions on the towfish have always been of interest (Chapman, 1982) since a ship in a sea state inevitably affects the towfish tethered to it. Some work has also been done on towfish interactions with the tow vehicle (Zhu and Li, 1997) but only at low speed. Cable dynamics tools like BCABLE (Wilkie, 1989) and DYNTOCABS (DYNamics of TOwed CABle Systems, Kamman et al., 1989, 1990, 1996) are successfully used to model tow cable systems. These programs do not model the tow vehicle because it is generally much more massive than the towfish, so little interaction occurs.

The emphasis in this paper is to develop a simulation tool with which to carry out interaction assessments, and do a preliminary assessment of one required maneuver. The interaction analysis is best done with a fully integrated drone/tow system simulator, a tool unavailable to the authors. To get preliminary results quickly, and assess the need for a fully integrated simulator, the analysis was carried out by iterating between two simulation packages that were available: the in-house DREA Submersible Simulation Program (DSSP) still in development, and DYNTOCABS. DSSP integrates the 6 degree-of-freedom equations of motion (Abkowitz, 1969) to obtain the vehicle state vector in response to a series of commands and external forces. DYNTOCABS determines the towfish and cable state vectors in response to a given towpoint trajectory.

Minehunting operations consist of towing the sonar back and forth to scan consecutive swaths of area. This requires periodically reversing the direction of the entire tow system. The U-turn is the simplest maneuver with which to do this but it results in large towfish positional displacements and large side forces that create large rolling moments on the tow vehicle. Although the sonar does not scan during a turn, it is still necessary to keep the towfish safely off the sea floor and to minimize the above effects while achieving steady state conditions on a reciprocal heading as quickly as possible. Large turning diameters reduce drone side force but take longer. Natural 'overshot' U-turns are shown to be a good compromise between these competing demands.

2. DYNAMICS MODELLING

2.1 Drone Dynamics (DSSP)

DSSP performs a time domain maneuvering simulation by numerically integrating the 6 degree-of-freedom equations of motion for an underwater vehicle (Abkowitz, 1969). The drone starts neutrally buoyant in level trim with a steady forward speed. At arbitrary time intervals, control surface deflection, ballasting, flooding, and propulsion changes are applied. Special modifications were made in DSSP to accomodate differentially deflecting aft planes (for roll control), to implement DOLPHIN-like autopilots for depth, heading, pitch and roll control (Seto, 1998b), to process and apply cable tensions to the towpoint (Seto, 1998a), and to model the DOLPHIN Mk2 hydrodynamic characteristics and propulsion system.

Active first order control algorithms are used for pitch, depth (heave), heading, and roll control. The system responds to errors in these quantities and their rates (the first time derivative of the error). The aft planes control pitch and roll and the foreplanes control depth. On older DOLPHINs, differentially deflecting foreplanes were used for roll control (Watt et al., 1997).

Drone added mass (Watt, 1988) and viscous forces and moments are modelled conventionally in the equations of motion using both linear and nonlinear hydrodynamic coefficients. The coefficients are estimated with standard methods used by DREA and are drawn from both theoretical and empirical means (Watt et al., 1997).

The propulsion model simulates the time dependent propulsion forces exerted on the vehicle throughout a maneuver in which engine rpm, vehicle velocity and direction may be continually changing. Included in the model are:

1) thrust/power as a function of vehicle speed, crossflow angle, and commanded and current rpm;
2) engine power limitations as a function of rpm;
3) engine rpm time response when an rpm command change is made.

The rpm time response prediction is based on a standard, second order control system model (Watt, 1990) that is also used for modelling other control functions in the vehicle, such as control surface deflection dynamics.

DYNTOCABS predicted tow cable forces are applied to the drone using DSSP's capability to model arbitrary, time dependent, external forces acting on the drone at arbitrary locations. However, a time history of these forces must be fully specified at the start of the simulation, making it necessary to iterate between the two programs.

Sea state and free surface effects are currently not modelled in DSSP. These can be simulated by using DSSP's external force capability, but have not yet been implemented.

2.2 Cable Dynamics (DYNTOCABS)

The three-dimensional, finite difference, unsteady cable code DYNTOCABS, developed by Kamman (Kamman et al., 1989, 1990, 1996) at Coastal Systems Station, Panama City, simulates the cable/towfish dynamics. The cable is modelled by a series of rigid links connected in a chain with frictionless spherical joints to simulate a flexible cable. The 3-component inertial, fluid and gravitational loads are assumed to be uniformly distributed over each link. These loads are halved and concentrated at connecting joints.

DYNTOCABS models the towfish as a six degree-of-freedom body with mass and inertia. An arbitrary reference point on the fish is connected to the last cable link by a frictionless spherical joint. The DYNTOCABS towfish model is described below.

The parameters specified for each cable link are length, diameter, weight, buoyancy, hydrodynamic loading functions (force distributions), initial steady state orientation angle guesses, and time derivatives of these guesses. The Folb-Nelligan hydrodynamic loading functions (no side force) for armoured tow cable were used (Casarella and Parsons, 1970). The boundary conditions required for DYNTOCABS include an acceleration time history specification for the tow point (at the drone).

DYNTOCABS proceeds by first carrying out a steady state analysis on the input configuration which results in a correct steady state cable profile and towfish attitude. It then propagates the maneuver with a nonlinear time domain analysis. As it is a boundary condition, the towpoint acceleration specification is rigidly adhered to. The output from DYNTOCABS includes the tow point tensions as a function of time. The resolution in time of this data can be as high as necessary. Generally, an output interval of about 0.5 second is enough for a 10 knot maneuver though the DYNTOCABS integration is performed every 0.01 seconds.

2.3 Towfish Dynamics (DYNTOCABS)

In DYNTOCABS, the towfish dynamics are modelled through a set of 55 linear and nonlinear hydrodynamic coefficients which are incorporated in equations of motion similar to those solved by DSSP. Minor modifications were made to this model to accomodate additional nonlinear viscous damping coefficients and additional active control surfaces required by the current towfish. The towfish hydrodynamic coefficients were estimated using the same methods as for the drone.

The current towfish has a large, active depressor which takes the fish to, and maintains, depth. The fish also has four active aft planes that share control authority for roll, pitch, and yaw. Roll control can be implemented either by yawing with the rudder (to keep the fish aligned with the tow) or by generating a torque through differential plane deflections. Both methods were used, with emphasis on the former. PID controllers are used in real life and implemented in these simulations. The towfish is approximately neutrally buoyant. It is equipped with an inertial navigation unit which provides the unsteady roll, pitch, and yaw error and error rate signals. A depth transducer gives depth error.

A classical linearized stability analysis was applied to the towfish, assuming a fixed, constant velocity towpoint. This showed the fish to be stable in yaw and roll but unstable in pitch. The analysis predicted that the instability could be eliminated by moving the towpoint forward about 15% of the towfish length. However, since the towfish simulation uses active pitch and depth control, pitch instability was never a problem and the tow point was not moved for the simulations carried out for this paper.

3. COMBINED DRONE/TOW SYSTEM MODEL

The procedures described here are for simulating a U-turn with a simple 'square wave' rudder deflection profile. The rudder is deflected to a constant value δ_r at $t = 0$ and back again to zero at $t = t_s$. These procedures will need to be modified for different maneuvers.

The iteration between DSSP and DYNTOCABS is coordinated in a Maple* worksheet. A combination of Maple procedures and executable fortran programs are called from this worksheet, with plotting of variables available within the worksheet. The iteration proceeds as follows:

1) An initial drone trajectory is established using DSSP and assuming tow cable tensions are zero. This establishes the rudder commands and their timing (the 'command profile') that give a turn with a nominally correct lane spacing (assuming the drone is trying to follow a survey grid).
2) A three dimensional inertial reference frame representation of the drone tow point trajectory as a function of time is fitted with cubic splines and differentiated twice to form the tow point acceleration time history profile input to DYNTOCABS. Second order acceleration profile splines are the usual DYNTOCABS input. DYNTOCABS was modified to accept this input at arbitrarily high densities in order to capture even small scale nuances in drone motion (Seto, 1998a). The splined tow point trajectory data is typically recorded every half second for a drone speed of 10 knots.
3) DYNTOCABS is run and outputs three component tow point tension at pre-determined time increments (about every half

* Waterloo Maple Inc., www.maplesoft.com

second) along the vehicle trajectory. This output is splined and transformed to the drone body axes, forming the input to the next iteration with DSSP. Before proceeding with the next DSSP iteration, however, the rudder command profile must be adjusted to deal with the changed cable tensions.

4) For the first iteration only, the rudder deflection needed to offset the tow is approximated from linearized versions of the lateral force and yawing moment equations of motion:

$$\delta_r = \frac{r'[Y_v'(m'x_G' - N_r') + N_v'(Y_r' - m')] + T_y'(N_v' - Y_v'x_t')}{Y_v'N_{\delta_r}' - N_v'Y_{\delta_r}'}.$$

Here, the average lateral body force cable tension, T_y, is an external force added to the equations of motion at the tow point x_t. The desired yaw rate $r' = r\ell/U$ is that from the initial DSSP calculation in step 1. The remaining terms are hydrodynamic coefficients. For subsequent iterations, a quasi-Newton iteration scheme is used to iterate the rudder deflection towards an angle that gives the desired yaw rate, r_0:

$$\delta_{r,i} = \delta_{r,i-1} + \frac{(\delta_{r,i-1} - \delta_{r,i-2})(r_0 - r_{i-1})}{r_{i-1} - r_{i-2}}.$$

5) The time, t_s, at which the rudder is re-zeroed to exit from the turn is chosen so the final vehicle heading is $\psi_f = 180°$. This proceeds as follows: $t_{s,1} = t_{s,0} + \Delta t$, $t_{s,2} = t_{s,1} + \Delta t$, where Δt is nominally 10 seconds (this has little effect on the final result) and, for subsequent iterations:

$$t_{s,i} = t_{s,i-1} + \frac{(t_{s,i-1} - t_{s,i-2})(180 - \psi_{f,i-1})}{(\psi_{f,i-1} - \psi_{f,i-2})}.$$

6) This double iteration in δ_r and t_s only converges if the two variables are iterated separately. Thus, the first DSSP/DYNTOCABS δ_r iterations are carried through to a converged trajectory before the first t_s iteration takes place. The iterations are redone with $t_{s,1}$ (but are faster because the trajectory does not change prior to $t = t_s$) and redone a second and third time with $t_{s,2}$ and $t_{s,3}$. The $t_{s,3}$ iteration results in an accurate $\psi_f = 180°$ heading because, with the tow system turn rate at $t = t_s$ almost steady state, ψ_f is a linear function of t_s as assumed in the above formula for $t_{s,i}$.

About 8 DSSP/DYNTOCABS iteration cycles are required with $t_{s,0}$ and 5 with each of $t_{s,1}$ through $t_{s,3}$. The total iteration takes about 1.5 hours on a Pentium (166 MHz) personal computer. Trajectory convergence is assumed when the largest difference in the trajectories from two consecutive iterations is about 0.001 m.

4. MODEL VALIDATION

No data exists for this particular cable and towfish system yet. However, DOLPHIN/towfish sea trials are planned to acquire data for validating the simulator.

The simulation can be compared with an ISER in-house, steady-state, two-dimensional empirical/analytical model of a towed system (that does *not* account for drone/towfish interactions). This program has been tuned and calibrated over the years and is a reliable predictor of steady state straight and level flight tow system characteristics. For 300 m of cable scope, the towpoint moving at 10 knots, and a towfish maintaining 100 m depth, the comparison yields:

Quantity	2D Steady State	Current Model
towfish depressive force (N)	7330	7490
DOLPHIN axial tension (N)	8940	8960
DOLPHIN normal tension (N)	1340	1250
towfish/drone axial separation (m)	269	270

This is good agreement.

5. RESULTS

The interaction simulation was applied to the DOLPHIN/cable/towfish system for U-turn maneuvers, as shown in Figures 2 through 6. Results are preliminary but do show how much interaction is present and highlight the considerations involved in towing a large fish.

Figure 2 shows the predictions for a non-interacting (ie, 0^{th} iteration) drone and active towfish going through a 400 m diameter U-turn at 10 knots with 300 m of cable and a 100 m deep towfish. Towfish depth keeping is good, pitch and roll angles are within 3 degrees of zero, and the tow-off angle at the drone (the angle the tow cable is pulled away from the drone's vertical plane of symmetry, as seen in planform) is as large as 20 degrees. Interestingly, though the tow point turn is complete in about 2 minutes, cable tensions do not reach steady state values until another minute has elapsed, presumably because the cable dynamic time constants are long (the cable is still settling to a new equilibrium).

Figure 3 shows the converged, fully interactive maneuver that results from the Figure 2 initial conditions. The rudder angle required to produce Figure 3 was a factor of two larger than that used in Figure 2. The overshoot at the end of the Figure 3 trajectory results from the tow-off force continuing to pull the drone inwards even though the rudder has been zeroed. Figure 4 shows the effect of the t_s iterations on final heading.

It is expected that the overshoot could be eliminated in this trajectory with an appropriately chosen continuously varying rudder command profile. However, the overshoot characteristic is desirable. It gets the cable behind the drone more quickly than the simple U-turn, as demonstrated below.

Other convergence schemes are possible but have not been pursued at this time. Presumably one can be found which gives identical lane spacing for the 0^{th} and final iterations. The main objective here was to generate full interaction solutions and examine the magnitude of the effect. For this, comparisons between 0^{th} iteration and converged trajectories should be made for runs with the same lane spacing. This is done in Figures 5 and 6.

A relevant operational survey issue is how long it takes the towfish to complete its turn and begin scanning another swath. Figure 5 compares the towfish trajectory from the interactive model (Figure 3a) to that for a 0^{th} iteration U-turn similar to Figure 2a but with the same lane spacing as in Figure 3a. The iterated model gets the towfish on track faster because it incorporates overshoot.

A comparison of 0^{th} iteration and fully interactive cable tensions at DOLPHIN's towpoint show small changes in form and magnitude (Figure 6a,c,e). These mainly reflect the difference in time at which the rudder is zeroed. Some difference in the lateral tension (Figure 6c) occurs as the interactive DOLPHIN goes through the turn.

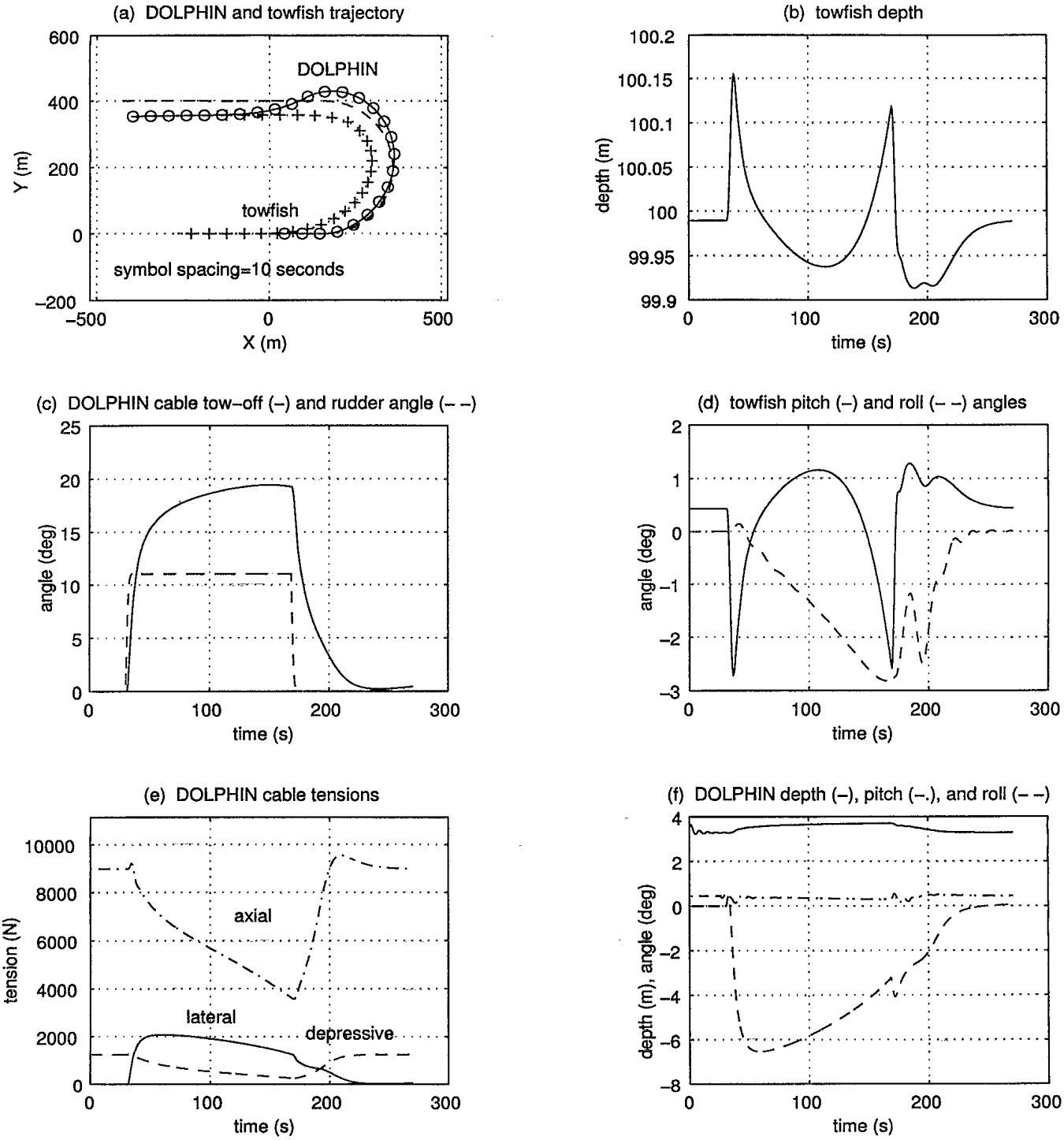

Fig. 3 *Converged interactive simulation with rudder re-zeroed at t_s = 168 seconds.*

further validation is required and full scale trials currently underway will allow this.

A preliminary examination of the interaction dynamics during U-turn trajectories using a simple rudder command profile has been presented. These interactions have a significant effect on the tow system trajectory and its evolution in time. Modelling them has led to a natural way of turning incorporating overshoot which brings the towfish back on track more quickly than occurs with a simple U-turn.

This work has shown that interaction effects for DOLPHIN and its towfish are significant; they will likely be larger with longer, deeper tows. Since the current iterative approach to solving for these effects is computationally intensive, and requires customized convergence algorithms that are trajectory dependent, a fully integrated drone/cable/towfish dynamic simulation eliminating iteration is desirable. This is particularly true when waypoint line-following modes and complex trajectories are considered.

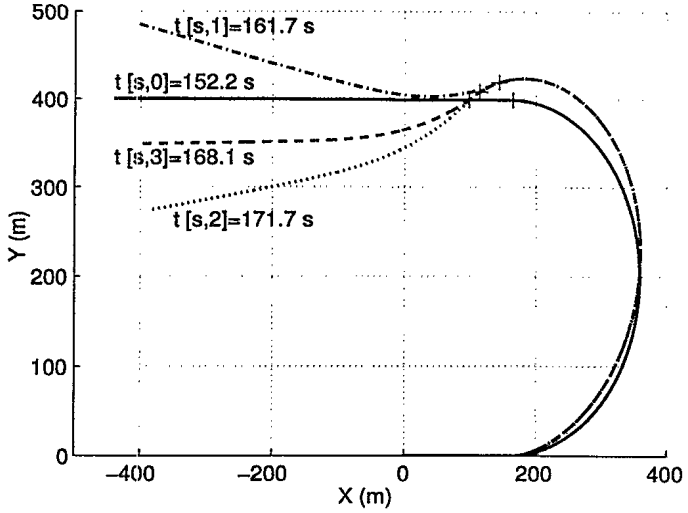

Fig. 4 *Converged interactive trajectories for the 0^{th} through 3^{rd} t_s iterations employed to get the Figure 3 results. The + symbol on a trajectory indicates where the rudder was re-zeroed.*

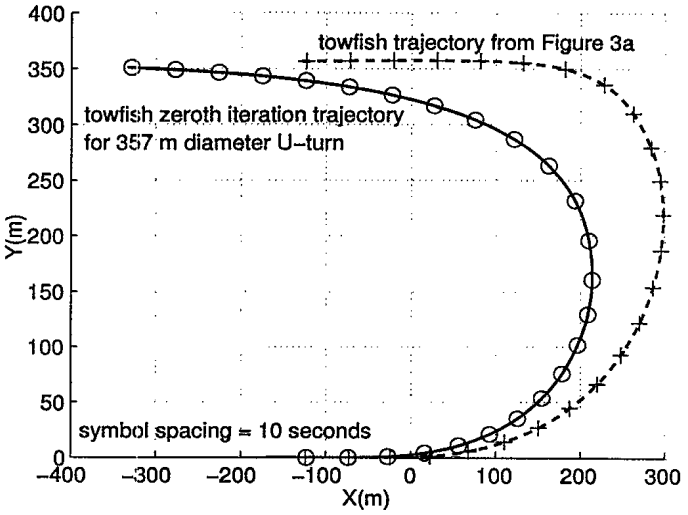

Fig. 5 *A comparison of 357 m wide towfish U-turns.*

Nevertheless, the current approach can be successful for simulating the simple trajectories common in route surveying. Indeed, work is underway to use the current method to assess the towfish response to drone surge induced by heavy sea states during straight line surveys.

ACKNOWLEDGEMENT

Mr. Mike Mackay of DREA is the main developer of the DREA in-house underwater vehicle simulator and hydrodynamic force predictor.

REFERENCES

Abkowitz, MA (1969). *Stability and Motion Control of Ocean Vehicles*. MIT Press.

Casarella, MJ, Parsons, M (1970). "Cable Systems Under Hydrodynamic Loading," *Marine Technical Society Journal*, Vol. 4, No. 4, pp. 27–44.

Chapman, DA (1982). "Effects of Ship Motion on a Neutrally-Stable Towed Fish," *Journal of Ocean Engineering*, Vol. 9, No. 3, pp. 189–220.

Chapman, DA (1984). "Towed Cable Behaviour During Ship Turning Maneuvers," *Journal of Ocean Engineering*, Vol. 11, No. 4, pp. 327–361.

Duvat, G, and Large, C (1997). "Experimental Study of the Dynamic Behaviour of a Towed System," *Proceedings of the Seventh International Offshore and Polar Engineering Conference*, Honolulu, USA, Vol. II, pp. 17–25.

Le Guerch, E (1987). "The Deep Towing of Underwater Fish Behaviour Patterns During Half-Turn Manoeuvres," *Ocean Engineering*, Vol. 14, No. 2, pp. 145–162.

Henry, C (1985). "On Optimum Turning Configurations with Fixed-Fin Stabilization," *IEEE Journal of Oceanic Engineering*, Vol. 20, No. 4, pp. 268–275.

Kamman, JW, Nguyen, TC and Crane, JW (1989). "Modelling Towed Cable System Dynamics," *Proceedings of the IEEE/MTS Oceans 1989 International Conference on Methods for Understanding the Global Ocean*, IEEE, New York, pp. 1484–1489.

Kamman, JW, Nguyen, TC (1990). "User's Manual for DYNTOCABS," Technical Memorandum NCSC TM 550–90.

Kamman, JW (1996). "Application of Multivariable Linear Control Design to Marine Towed System," *Journal of Guidance, Control and Dynamics*, Vol. 19, No. 6, pp. 1246–1251.

Preston, J and Shupe, L (1993). "Remote Mine-Hunting Systems — Vehicle Stability Trials," *Proceedings on the Knowledge-Based Systems and Robotics Workshop*, Fisheries and Oceans Canada, pp. 115–121.

Seto, ML (1998a). "Interactive Model for DOLPHIN Towing a Towfish," ISER report in press.

Seto, ML, (1998b). "Adapting the DREA DSSP for a 6 Degree-of-Freedom Dynamic Simulation of the Semi-Submersible DOLPHIN," ISER report in press.

Watt, GD (1988). "Estimates for the Added Mass of a Multi-Component, Deeply Submerged Vehicle," *RINA Warship 88 International Symposium on Conventional Naval Submarines*, paper no. 14.

Watt, GD (1990). "Modelling Submarine Control Surface Deflection Dynamics," DREA Technical Memorandum 90/203.

Watt, GD, Seto, ML, Brockett, TE (1997). "Hydrodynamic Considerations for Semi-Submersible Minehunting Vehicles," *Proceedings of the 4^{th} Canadian Marine Hydromechanics and Structures Conference*, Ottawa.

Wilkie, M (1989). "User's Guide to BCABLE," DREP Contractor Report 89–5.

Zhu, K, and Li, W (1997). "Coupled Motion Simulation of Underwater Towed and Self-Propulsive Vehicle," *Proceedings of the Seventh International Offshore and Polar Engineering Conference*, Honolulu, USA, Vol. II, pp. 38–43.

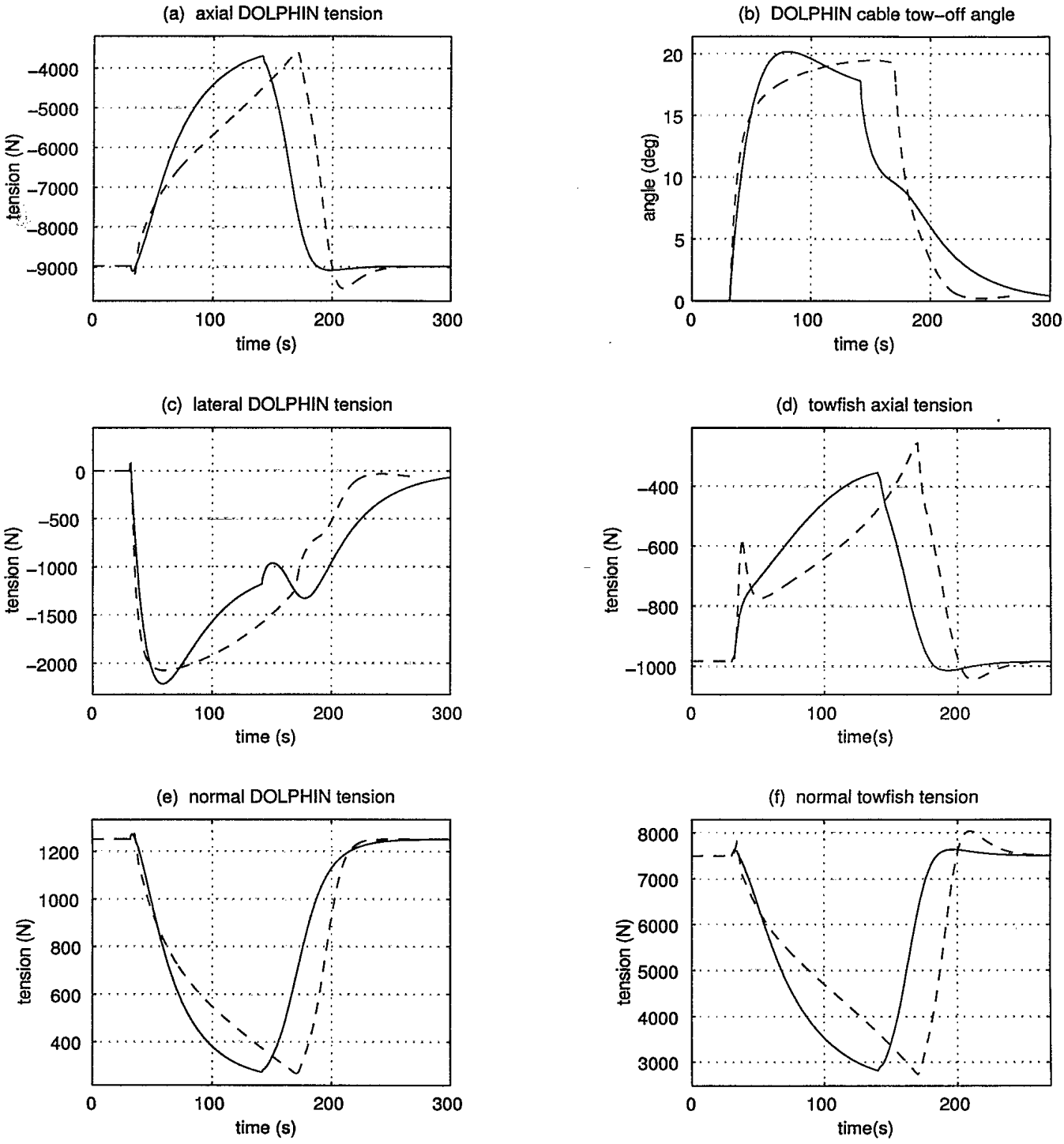

Fig. 6 *Cable tension levels at DOLPHIN's towpoint and the towfish for the 357 m turns shown in Figure 5: converged interactive (– –) and 0^{th} iteration (—) tension components.*

#508292